ARTICLE IN PRESS

Materials Science and Engineering A xxx (2004) xxx–xxx

MATERIALS SCIENCE & ENGINEERING A

www.elsevier.com/locate/msea

Rapid solidification behaviour of undercooled levitated Fe–Ge alloy droplets

K. Biswas [a], G. Phanikumar [a,b,*], K. Chattopadhyay [a], T. Volkmann [b], O. Funke [b], D. Holland-Moritz [b], D.M. Herlach [b]

[a] *Department of Metallurgy, Indian Institute of Science, Bangalore, India*
[b] *Institute for Space Simulation, German Aerospace Centre, Cologne, Germany*

Abstract

The solidification behaviour of $Fe_{82}Ge_{18}$ and $Fe_{75}Ge_{25}$ alloys is studied by using an electromagnetic levitation facility. The maximum undercooling attained in the case of $Fe_{82}Ge_{18}$ alloy is 240 K. Growth velocity of α- (bcc) phase is measured using a photodiode technique and shows two distinct regimes. In the case of $Fe_{75}Ge_{25}$, the maximum undercooling attained is 165 K. At low undercoolings two recalescence events occur, corresponding to formation of α- and ε-phase (DO_{19}). At large undercoolings the peritectic reaction (α + liquid → ε) is suppressed. Microstructural analysis indicates morphological changes in the microstructure as well as a competition among phases nucleating at different levels of undercooling.

Keywords: Rapid solidification; Undercooling; Levitation; Phase selection; Fe–Ge

1. Introduction

Undercooling experiments on liquid metals are an attractive method to study crystal growth phenomena under non-equilibrium conditions and their influence on the formation of metastable solid states. The conditions of rapid solidification of bulk undercooled samples concern both deviation from chemical equilibrium at the solid–liquid interface and kinetic undercooling of the interface [1]. The non-equilibrium conditions at the solidification front control the solidification of a great variety of solid phases far from equilibrium. Such metastable solids range from metastable crystalline phases over supersaturated solid solutions and grain-refined alloys to disordered superlattice structures in intermetallic compounds [2].

The binary alloy system of Fe–Ge comprises of several critical points and order–disorder phase transitions. Phase selection and microstructure formation is not completely understood in this system and the literature on these studies is limited [3,4]. Due to the presence of several critical points in the phase diagram, the system exhibits ordering and clustering reactions and offers exciting possibilities in microstructure design. The phase diagram of the Fe–Ge system [5] (Fig. 1) indicates that the compositions chosen, $Fe_{82}Ge_{18}$ and $Fe_{75}Ge_{25}$, are within the range of intermetallic phase formation and exhibit ordered phases up to the liquidus temperatures. The alloy composition near $Fe_{82}Ge_{18}$ is reported to exhibit a two stage ordering process of $\alpha(\text{disorderedbcc}) \rightarrow \alpha_2(B2) \rightarrow \alpha_2(B2) + \alpha_1(DO_3)$. The equilibrium solidification of $Fe_{75}Ge_{25}$ composition starts with nucleation of ordered $\alpha_2(B2)$. The ordered hexagonal phase $\varepsilon(DO_{19})$ then forms via a peritectic reaction between α_2 and the remaining liquid at 1163 °C. The ε-phase is dimorphic and the transformation $\varepsilon(DO_{19}) \rightarrow \varepsilon'(L1_2)$ occurs at 700 °C and is sluggish [5–7]. Thus, non-equilibrium processing offers a possibility of retaining the intermetallic phases in disordered structures in this system.

2. Experiments

Alloy samples of about 6–8 mm diameter are prepared by arc-melting from 99.99% pure Fe and 99.999% pure Ge. Undercooling experiments are carried out using an electromagnetic levitation set-up [8]. The chamber is evacuated to 10^{-4} mbar before backfilling with 800 mbar He—4 vol.% H_2 gas of 99.999% purity. The samples are undercooled in

* Corresponding author.
E-mail address: phanikumar.gandham@dlr.de (G. Phanikumar).

0921-5093/$ – see front matter
doi:10.1016/j.msea.2003.10.047

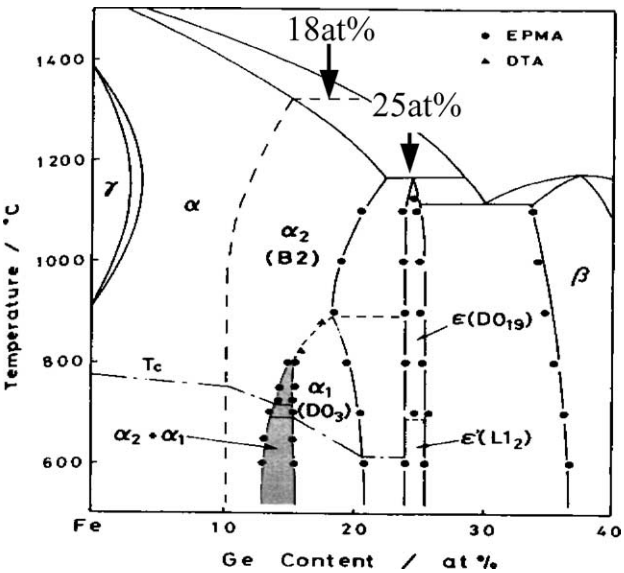

Fig. 1. A portion of the Fe–Ge phase diagram showing the compositions under study.

a containerless fashion to a predetermined temperature and solidification is triggered externally by touching the liquid droplet with an alumina needle. Photodiode technique [9] is used to measure the growth velocity of the solid phase as a function of undercooling. X-ray diffraction is used to identify the phase mixture of the bulk samples. Since the superlattice reflections are of low intensity, ordered nature of the phases could not be concluded and the phases will be referred by the corresponding disordered ones. Composition analysis using an Oxford EDX attachment to the scanning electron microscope (Jeol JSM 840-FX) is used to identify the individual phases in a given microstructure.

3. Results and discussion

3.1. $Fe_{82}Ge_{18}$ alloy

Fig. 2 shows growth velocity as a function of amount of undercooling for the $Fe_{82}Ge_{18}$ alloy. The growth velocity

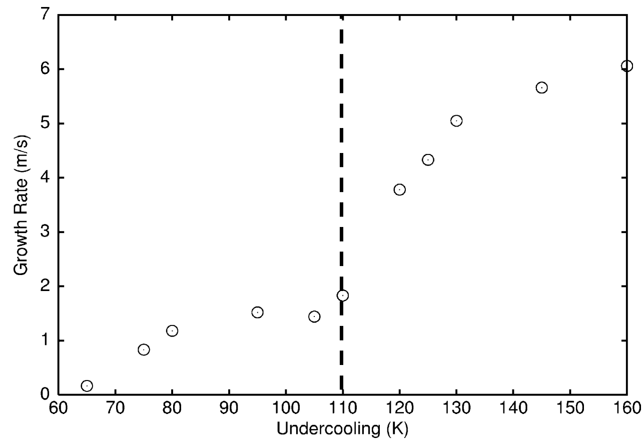

Fig. 2. Growth velocity as a function of undercooling for $Fe_{82}Ge_{18}$.

corresponds to that of α dendrites. There are two distinguishable regimes of this plot. At low undercooling, the nature of the curve is similar to the one described using dendrite growth theory. At undercoolings around 110 K, there is a sharp increase in the growth velocity. In alloy solidification, such a kind of transition is related to change of growth mode from predominantly solute controlled growth to thermal and solute controlled growth with an increasing undercooling level [10]. The slight drop in growth rate at 107 K is within the experimental error estimated to be around ±10%.

Samples were sectioned to observe microstructures under optical and scanning electron microscopes. The as-cast microstructure (Fig. 3a) exhibits large grains of single phase α. The microstructures of samples undercooled at different levels are shown in Fig. 4. The dark streaks in Fig. 4a are due to the ridges as seen by the optical microscope and are part of elongated dendrite fractions revealed due to deep etching. At low undercooling, the grains are elongated while samples with more than 110 K undercooling exhibit a finer equiaxed grain morphology (Fig. 4b–d). Grain-refinement at intermediate undercoolings is already explained recently [11]. This may be invoked for our observations as well. The sharp change in growth velocity as a function of undercooling also coincides with change in growth morphology from elongated

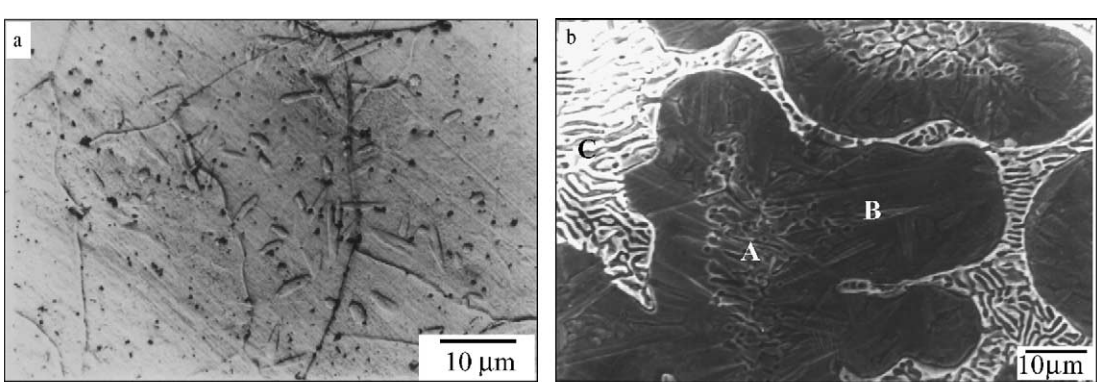

Fig. 3. As-cast microstructures of (a) $Fe_{82}Ge_{18}$ and (b) $Fe_{75}Ge_{25}$ alloys. The compositions in atom percent are A: Fe + 21.49Ge (α); B: Fe + 24.21Ge (ε); and C: Fe + 35.37Ge(ε + β eutectic).

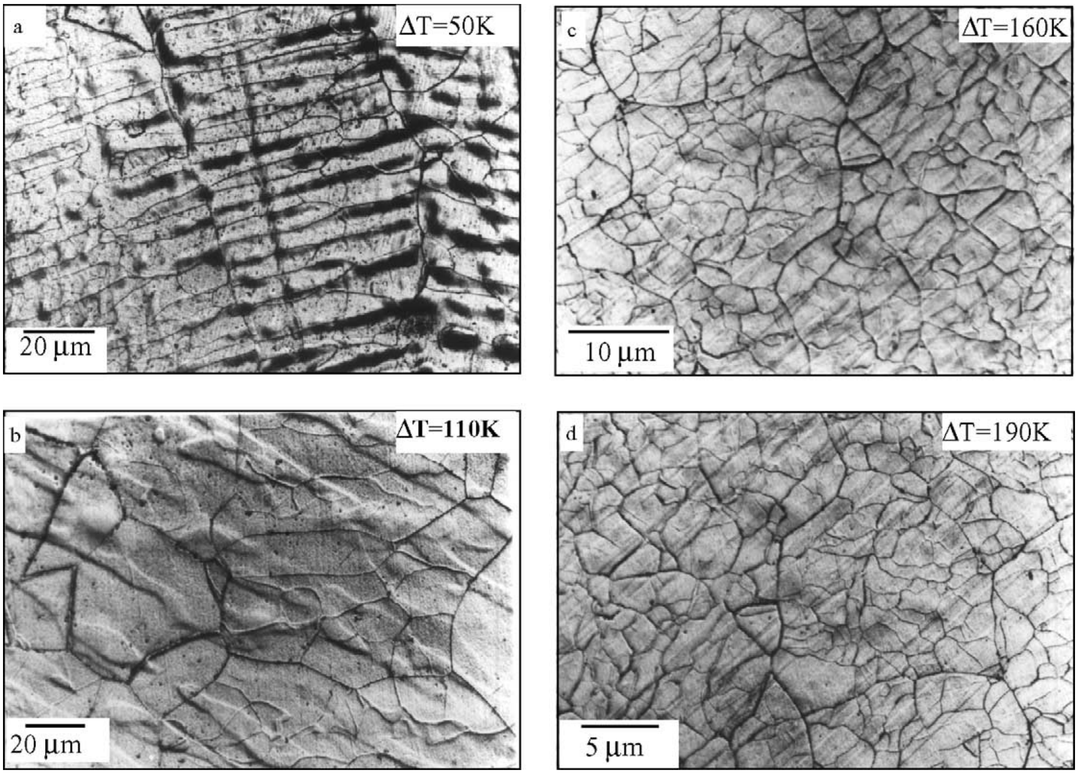

Fig. 4. Optical micrographs of $Fe_{82}Ge_{18}$ solidified at different undercoolings.

to grain-refined equiaxed microstructure. X-ray diffraction experiments did not reveal presence of superlattice reflections. However, the low intensity of these reflections requires an independent corroboration of disorder trapping.

3.2. *$Fe_{75}Ge_{25}$ alloy*

The microstructural evolution of $Fe_{75}Ge_{25}$ as function of undercooling is shown in Fig. 5. The microstructure of the

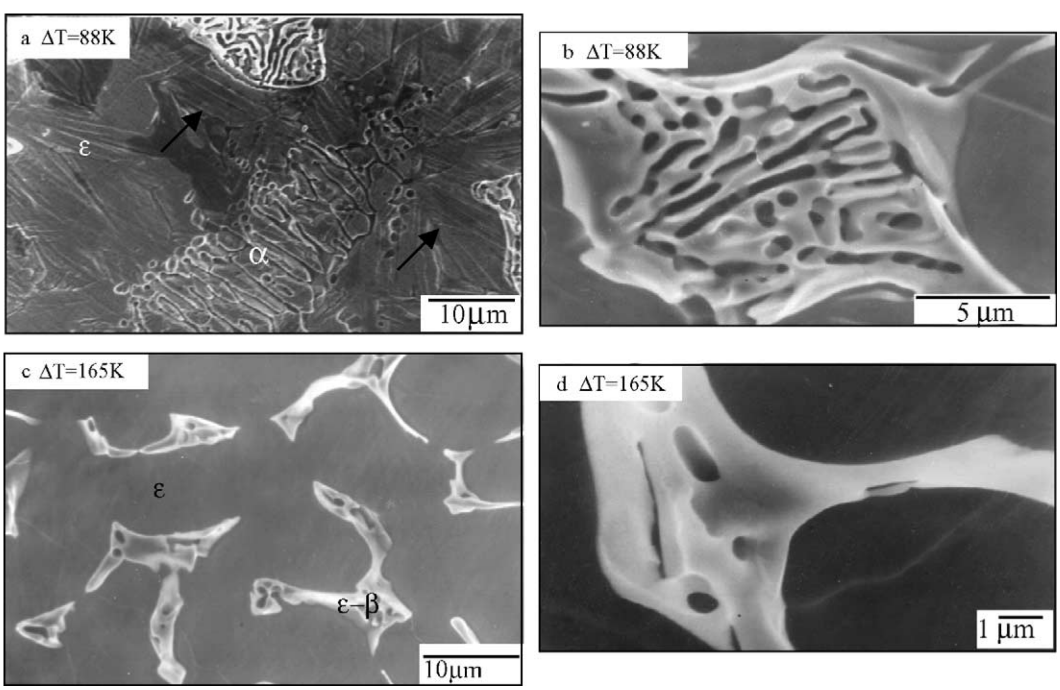

Fig. 5. SEM microstructures of $Fe_{75}Ge_{25}$ solidified at undercoolings (a,b) 88 K and (c,d) 165 K. Corresponding eutectic microstructure (β-white + ε-dark) are shown in b and d.

as-cast (Fig. 3b) and low undercooled (Fig. 5a) alloys reveals presence of three phases namely, α-, ε- and β-phases. The respective compositions are indicated in the figure caption of Fig. 3. The β-phase can be seen only as a eutectic of ε–β. The temperature–time curve (not shown here) for low undercooling experiments reveals two recalescence events separated by a time interval of nearly 10 s. We attribute the first event to α-phase formation and the second to ε-phase formation. In addition, presence of the α-phase embedded in ε grains with intergranular eutectic phase confirms occurrence and incompletion of the peritectic reaction [12]. The growth rate measurements for this composition are not discussed here due to want of space.

The solidification behaviour of alloys undercooled to 110 K and more is distinctly different. Scanning electron micrograph (Fig. 5c) shows the presence of only ε-phase without twins. The eutectic mixture of ε–β in the sample is minimal and the α-phase is absent. This indicates that either the nucleation of ε-phase was directly from the liquid state or the primary phase underwent a solid-state transformation. This possibility of suppressing the peritectic reaction is important in obtaining phase-pure intermetallic ε-phase. Recent in-situ diffraction experiments (not shown here) indicate that the primary phase to nucleate is α-phase even above 110 K, indicating that the solid-state transformation of super saturated α- to ε-phase is the likely possibility. Further work is needed to corroborate this speculation. The ε-phase shows growth of twins for low undercooled sample (indicated by arrows in Fig. 5a). These were not observed at higher undercoolings. The morphology of the eutectic ε–β also changes as a function of undercooling. The Fig. 5b and d show eutectic morphology in samples solidified at different undercoolings. As the undercooling is increased, the eutectic microstructure changes from lameller to rod morphology. The volume fraction of the eutectic phase continually decreases with undercooling, leading to nearly phase-pure ε microstructure and is an important outcome of the study.

4. Conclusions

The $Fe_{82}Ge_{18}$ alloy shows a change of grain morphology from elongated to fine equiaxed at undercoolings above 110 K. Growth rate of the α-phase as a function of undercooling is determined. The $Fe_{75}Ge_{25}$ alloy solidifies via a peritectic reaction at low undercoolings (<110 K) with the ε-phase showing growth of twins. At higher undercoolings, the peritectic reaction is suppressed and the final microstructure is nearly phase-pure ε.

Acknowledgements

The work derives support from a joint project from BMBF, Germany and DST, India.

References

[1] R. Willnecker, D.M. Herlach, B. Feuerbacher, Phys. Rev. Lett. 62 (1989) 2707.
[2] D.M. Herlach, Mater. Sci. Eng. A226–228 (1997) 348.
[3] B. Predel, M. Frebel, Z. Metall. 63 (1972) 393.
[4] K. Raviprasad, S. Ranganathan, K. Chattopadhyay, Scripta Met. et Mater. 26 (1992) 467.
[5] H. Enoki, K. Ishida, T. Nishizawa, Met. Trans. 18A (1987) 949.
[6] T.B. Massalski, H. Okamoto, P.R. Subramanian, L. Kacprzak, Binary Alloy Phase Diagrams 2 (1986) 1704–1706.
[7] Q.Z. Chen, A.H.W. Ngan, B.J. Duggan, Intermetallics 6 (1998) 1051.
[8] D.M. Herlach, Mater. Sci. Eng. R12 (1994) 177.
[9] E. Schleip, R. Willnecker, D.M. Herlach, G.P. Görler, Mater. Sci. Eng. A98 (1988) 39.
[10] W.J. Boettinger, S.R. Corriell, R. Trivedi, in: R. Mehrabian, P.A. Parish (Eds.), Rapid Solidification Processing: Principles and Technologies IV, Claitor's, Baton Rouge, 1988, p. 13.
[11] A. Karma, Int. J. Non-Equilib. Process. 11 (1998) 169.
[12] H.W. Kerr, W. Kurz, Int. Mater. Rev. 41 (1996) 129.